ANALYSIS OF BENDING MECHANICAL PERFORMANCE OF WELDING JOINTS WITH THE ADDITION OF DIAMOND AND CIRCULAR PLATES

GATOT PRAYOGO[1*], MUHAMMAD ARIF BUDIYANTO[1], MUSTASYAR PERKASA [2]

[1]Department of Mechanical Engineering, Universitas Indonesia, Kampus Baru UI, Depok, Jawa Barat-16424, Indonesia
[2]Laboratory of Structural Strength, Directorate of Laboratory Management, Research Facilities, and Science and Technology Park - National Research and Innovation Agency, B.J. Habibie Science & Technology Complex, Building 220, South Tangerang, Banten-15314, Indonesia

**Corresponding author: gatot@eng.ui.ac.id*

(Received: 2 February 2023; Accepted: 21 February 2023; Published on-line: 1 March 2023)

ABSTRACT: The design and analysis of welded joints are very useful for the safety of steel-based structures. The effect of welded joints meeting at one point on the resulting stress is a critical factor in constructing steel joints. The main objective of this research is to analyze the mechanical performance and microstructure of the welding process on diamond and circular plate joints. The analysis was carried out through experiments and finite element simulations to find out how much influence the addition of a diamond plate and circular plate had on the plate connection. The method used is to analyze the strength, hardness, and micro and macrostructure testing to determine the strength and structural changes of the metal after welding. The results of the test are then used to create an inhomogeneous model of weld joint, then the model is applied to the FEA software to be analyzed by the bending test simulation. The experimentally bending testing was carried out to examine bending performance of the test objects. From the simulation and experimental results, it is found that the shape of a circular plate measuring a diameter of 60 mm with a thickness of 6 mm is appropriate for a flat plate joint, and the flat-diamond plate measuring 60x60 mm with a thickness of 6 mm is proper for application to un-flat (cornered) plate joints. The structural integrity of a flat plate joint with a circular plate is greater than that of a diamond plate.

KEY WORDS: Welded joints, diamond plate, circular plate, and bending test.

1. INTRODUCTION

Welding is the process of joining two or more metal parts using heat energy. Welding can also be defined as a metallurgical bond at a metal alloy joint that occurs in a melted or liquid state, in other words welding is a local joining of two metals using heat energy [1]. Welding is an integral part of the manufacturing process [2]. Welding can also be defined as a metal joining technique by partially melting the base metal and filler metal with or without pressure and with or without additional metal and produces a continuous connection [3]. Welding of low-carbon steel is usually carried out using the SMAW (Shielded Metal Arc Welding) welding process [4]. Low carbon steel, also called mild steel, is easy to weld steel, can be welded by all welding methods available in practice, and the result will be good if the preparation is perfect and the requirements are met [5]. Low-carbon steel has good weldability compared to medium-carbon

steel and high-carbon steel [6]. Weld cracks that may occur in welding thick plates can be avoided by preheating or by using low hydrogen electrodes [7,8].

Welding can be more precisely said to be an area that is affected by heat input during the welding process [9]. Based on this definition, the weld consists of 3 main parts, namely the Fused zone (weld Metal), Bonding zone (fusion line), heat affected zone (HAZ) [10]. An important aspect of a welding that receives important attention from finite element simulation analysis is metallurgical transformation or phase transformation. The purpose of metallurgical calculations is to determine the percentage of individual phases exposed to heat in the zone [11].

Research on the physical properties of a metal is very important to study the microstructure of metals [12]. The physical properties of a metal include density, thermal properties, electrical conductivity, and magnetic properties. Mechanical tests that are usually carried out, such as tensile, hardness, impact, creep, and fatigue tests aim to check the quality of the resulting product based on a standard specification. Mechanical properties include tensile strength, hardness, ductility, toughness and yielding [13].

The mechanical properties of a welding result can be seen in the high energy density of the weld beam, which has certain characteristics such as single-pass welding where the liquid zone is narrow [14]. These characteristics will have an influence on the mechanical properties. Regarding the tensile test, the test results show that the tensile specimen generally breaks or breaks in the base metal area [15].

Hardness is a measure of a material's resistance to plastic deformation. Hardness generally expresses resistance to deformation and measures a metal's resistance to plastic deformation or permanent deformation [16]. Inhomogenous deformation and failure of welded joints and components is a problem for most manufacturing industries. There is a big difference between the mechanical properties of the base material and the material that has undergone the welding process, the evaluation of the mechanical properties of welded joints has become a hot topic in the research world [17].

The properties and material characteristics of welded joints have been modeled by evaluating the strength of the connection using a comparison function between the strength of the material and the geometric size of the HAZ [18]. The method used is Finite Element Method Analysis (FEM Analysis) on the tensile strength of the specimen by comparing the results of the distribution of tensile strength on a plate, to identify an analytical approach for predicting the tensile strength of the steel joint ratio [19].

In addition, research has been carried out on modeling inhomogeneous deformation and damage to aluminum alloy welded joints [20]. The experiment is carried out based on existing procedures, where there are two types of specimens to be tested: a homogeneous material and inhomogenous material such as the butt joint plate connection [21].

Based on the existing research gap, there is still not much discussion about meeting welded joints at one point to the generated stress. Applicative studies are needed that can be applied to welding joints that meet at one point, namely diamond plates and circular plates.

The main objective of this research is to determine and study the mechanical performance and microstructure change of the welding process on diamond and circular plate joints by comparing the experimental results to the simulation results of Finite Element Analysis (FEA) using commercial software. The results of this study provide benefits, namely knowing the changes in the micro-structure and macro-structure that occur in the material due to the welding process.

2. METHODOLOGY

2.1. Research Stages

This research stage begins with collecting data and sources regarding the welding process, testing the welding results and the material's characteristics before and after being welded. In general, the stages of this research are shown in Fig. 1. In addition to data collection, the next stage is material identification. In this study, ST42 material is used, then the welding process is carried out. After welding, the welded areas are identified by means of metallography on the cross-section of the existing specimens. Experiments were carried out by testing the weld specimen by following the ASTM standard [22]. FEA modeling is done using commercial software, which is then imported into ANSYS [23], then entering material data from the results of material identification and test data as well as existing literature data. There are two case studies used, namely diamond plate and circular plate.

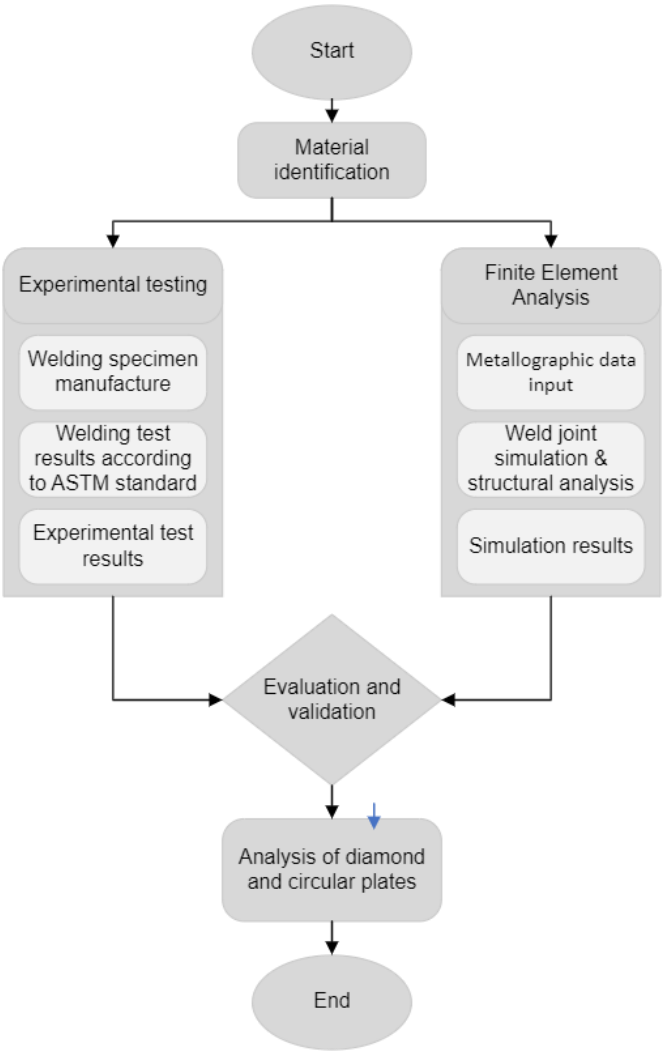

Fig. 1. Research stages.

2.2. Specimen Preparation

In this research, the test material used is an ST42 steel plate with a thickness of 6 mm. The electrodes used were ESAB, E 6013 with a diameter of 2.6 mm and 3.2 mm. The etching material used is 96% alcohol, 5 ml HNO_3 (Nital). Preparation of the ST 42 steel plate specimen

can be explained briefly as 1) the size of the material to be used for welding is 200 x 200 cm with a thickness of 0.6 cm, and 2) at the ends of the specimen to be joined by welding was machined to create a double V with an angle of 60° as shown in Fig. 2. The chamfer at the end of the specimen by 30° was machined using a milling machine and proved that the angle size is correct.

Fig. 2. ST 42 steel plate dimension.

The test object to be carried out in the welding process consists of several shapes of plates that have undergone a machining and preparation process. The test object is then arranged according to the meeting area of the sides to be connected through the welding process. The test objects can be seen in Fig. 3.

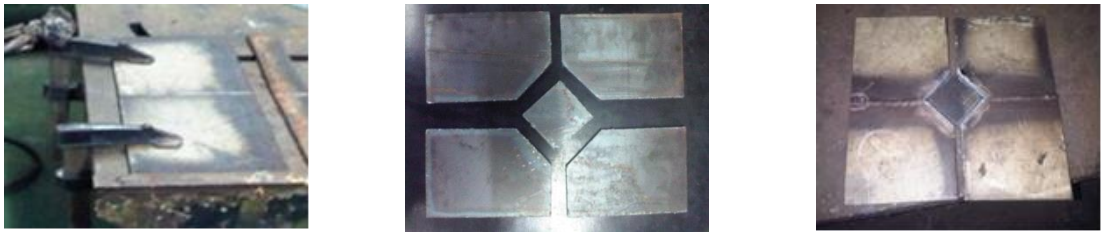

Fig. 3. Welding process on the test object material.

After preparing the test material, then the welding process using the SMAW method is performed, where during the rooting stage, the electrode diameter of 2.6 mm and current of 95 amperes are used. Then during the filling stage, the electrode diameter of 3.2 mm and current of 110 amperes are used. There are two types of welding routes on the test plate material, namely diamond and circular plate welding routes as shown in Fig. 4.

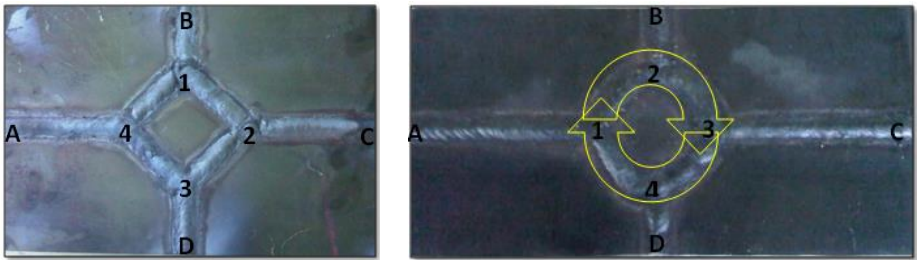

(a) (b)

Fig. 4. Two types of welding routes on the test plate material: (a) Welding route for diamond plate, and (b) Welding route for circular plate.

Welding Process Route:

A – 1: Welding the first stage,

B – 2: Welding the second stage,

C – 3: Welding the third stage,

D – 4: Welding the fourth stage

2.3. Testing Tool

The equipment used in this test is a welding machine, a set of metallography test equipment, tensile and bending test equipment as shown in Fig. 5. The welding machine used in this study is an electric arc welding machine with a current of 60 – 300 A, type of BXI – 300 – 2 PRIM VOLTAGE 380/200 V. A set of metallography test equipment consists of an Olympus Optical Microscope with type of MMB 2000, weight 17 kg, power supply 230 VAC, and a Nikon MM-40 macro measuring microscope. The test equipment used is the Shenck TREBEL universal testing machine.

Fig. 5. Equipment used micro and macro structure test equipment, tensile and bending test.

2.4. Metallography

The purpose of this test is to describe the microstructure change of the material due to the welding process. The steps of metallography testing are as follows, i.e., the surface of cross-section welded materials is gradually sanded with water-resistant sandpaper with flowing the water through it. The sandpaper sizes used are 220, 400, 800, 1000, and 1500. Then, performing the etching process which is carried out on the surface of test object according to the test standard of ASTM E 407. The etching tools needed are test tubes, measuring cups and pipettes, the etching material needed is Alcohol 96% HNO_3 5 ml.

The etched test object is placed on the anvil perpendicular to the microscope lens. After focusing the test object to the lens, taking photographs was carried out several times using magnification of 200 X to 500 X. Photographs were taken at four identified different locations on cross section of weld joint, i.e., the base metal area, the transition area, the HAZ, and the weld area.

Microhardness testing was also conducted in this research. This test aims to determine the hardness value of the welded joint material in several essential areas. The micro hardness testing was carried out based on Vickers method according to ASTM E92−17 hardness testing standard. The test is carried out with several stages and several test samples. The testing stage consists of taking microhardness data in areas that have been identified as HAZ, WELD, BASE MATERIAL areas. The second stage is taking the micro-hardness data in the middle area of the test specimen, where the data taken starts from the weld material area and is drawn in a straight line to the base material with a distance of 0.25 microns taking the microhardness

value. The hardness tested specimen can be seen in Fig. 13 and 14. Then the results of the microhardness test were converted to tensile strength values.

In this testing, distance measurement is also carried out to measure the distance between two very small points. In this measurement, it measured the distance between the HAZ region, the HAZ region to the weld core, and the HAZ region to the transition region. This test uses a Measuring Microscope with type MM-40 of Nikon.

2.5. Finite Element Analysis

Modeling of non-homogenous welding materials is carried out using CAD software, namely SOLIDWORK 2009 with an academic license. The initial data used to model the non-homogenous welding material was taken based on the results of distance measurements and macroscopic photos of the cross-section of the ST.42 ship plate material. Non-homogeneous modeling is done by idealizing macroscopic photo of cross-section of welding area and the test results of distance measurements. The modeling results are then applied to model the geometry of diamond, circular plate as well as butt joint model for the FEM simulation process using CAE software, namely ANSYS.

The butt joint, circular and diamond plate modeling were carried out using CAD software, namely Solidwork 2009. The butt joint model shown in Fig. 6 is welding flat plate material with the dimensions of the base material plate being 200 x 200 mm and 6 mm thick. Modeling is done by idealizing the existing butt joint welding results. The dimensions of the plate and the dimensions of the weld seam are considered ideal, consist of two plates with dimensions of 200x200 with a thickness of 6 mm, assembled together, and a root height of 1 mm, and a camper of 30°.

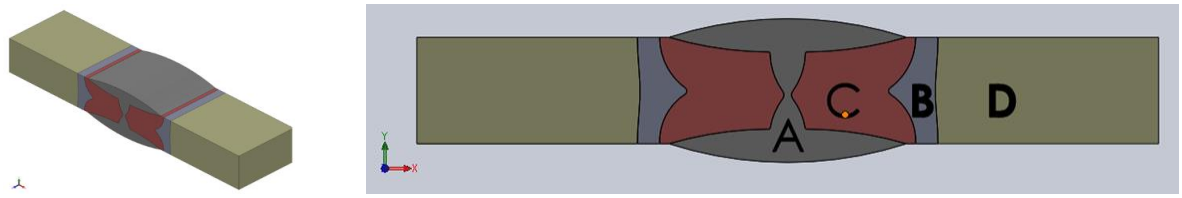

Fig. 6. Inhomogeneous of double V welded butt joint model.

Where: a is wed material, b is HAZ fine grained, c is HAZ coarse grained, and d is base material.

The diamond and circular plate models were shown in Fig. 7. The diamond plate model has dimensions of 60 mm with a plate thickness of 6 mm. A circular plate model has with a diameter of 60 mm and a thickness of 6 mm. The results of the modeling then proceed to the FEM simulation process using CAE software, namely ANSYS 14, of an academic license.

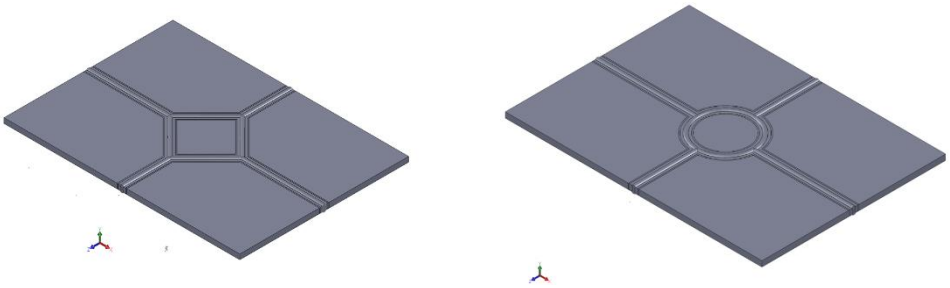

Fig. 7. Diamond and circular plate simulation models.

The geometry model that has been made into a solid model is then carried out in the FEM simulation process. After being imported into ANSYS then discretization (meshing) is carried out on the model as shown in Fig. 8. Then, inputing inhomogenesous material data based on the results of microstructure analysis and test standards were carried out. The input material data is as shown in Table 1.

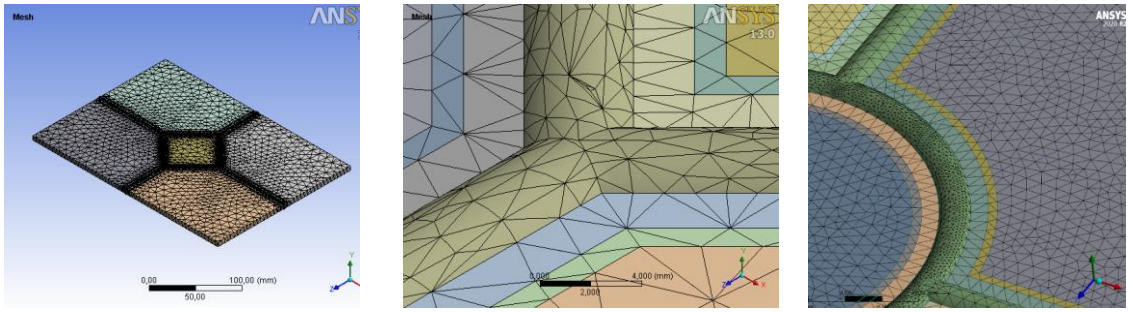

Fig. 8. Discretization (meshing) simulation model.

Table 1: Technical Properties of the welded area Material

Properties	Weld Material	Base Material	HAZ Coarse	HAZ Fine
σ_s (Mpa)	581,035	502,491	570,826	497,878
σ_y (Mpa)	484,196	418,743	475,689	414,898
Poison ratio (J)	0,3	0,26	0,3	0,3
ρ (kg/mm3)	7,85 E-06	7,85 E-06	7,85 E-06	7,85 E-06
Ê (Pa)	2,016 E+11	2,016 E+11	2,016 E+11	2,016 E+11

The illustration of the boundary conditions given to the model can be seen in Fig. 9.

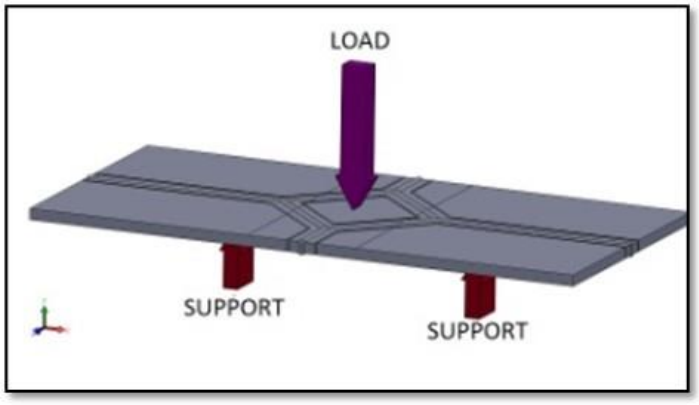

Fig. 9. Boundary conditions simulation model.

2.6. Verification and Validation

In order to ensure the simulation results delivered are valid, two stages called verification and validation were performed during the FEM simulation. The first stage was verification of the simulation model using the grid independence test to ensure that the number of meshes used gave consistent results. The results of the grid independence tests in this FEM simulation are shown in Fig. 10, Fig. 11, and Fig. 12. From these results, the mesh used in this simulation was a fine mesh with a mesh count around of 500,000, where the independence test graph shows that the maximum stress result was constant and that there was no significant change. Based on these results, it can be determined that the number of meshes used was appropriate. From the results of the tensile test and the simulation of the Butt Joint tensile test, the results obtained are as shown in Fig. 13. The simulation results are taken by observing the area that experiences the highest stress in the area that breaks during the tensile testing process so that the percentage value from the simulation and experimental results is a maximum of 7.2% where is at a maximum force of 51 kN consistent with the previous research [26].

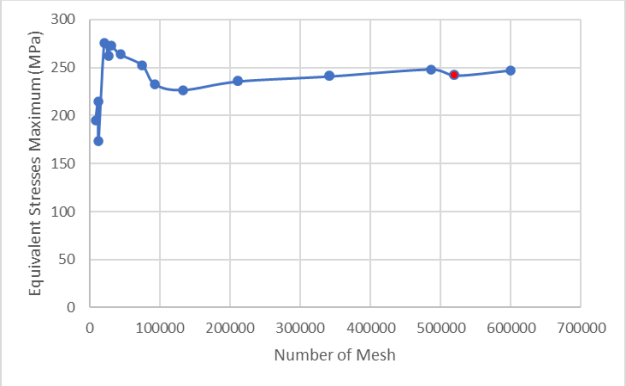

Fig. 10. Grid independence test of simulation model for plate welding joint with addition of circular plate.

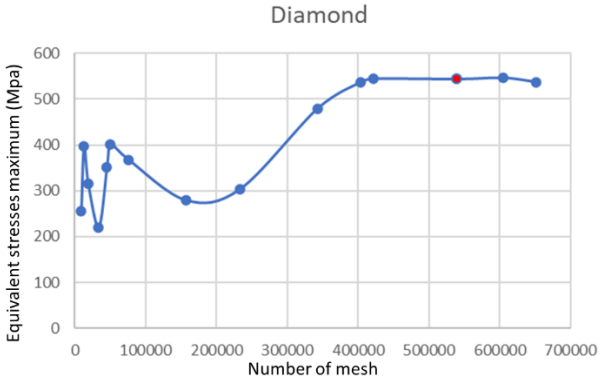

Fig. 11. Grid independence test of simulation model for plate welding joint with addition of diamond plate.

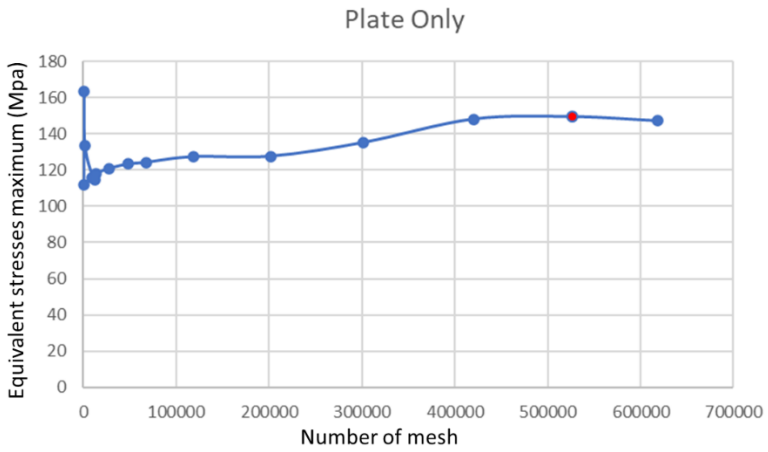

Fig. 12. Grid independence test of simulation model for base plate only (without welding joint).

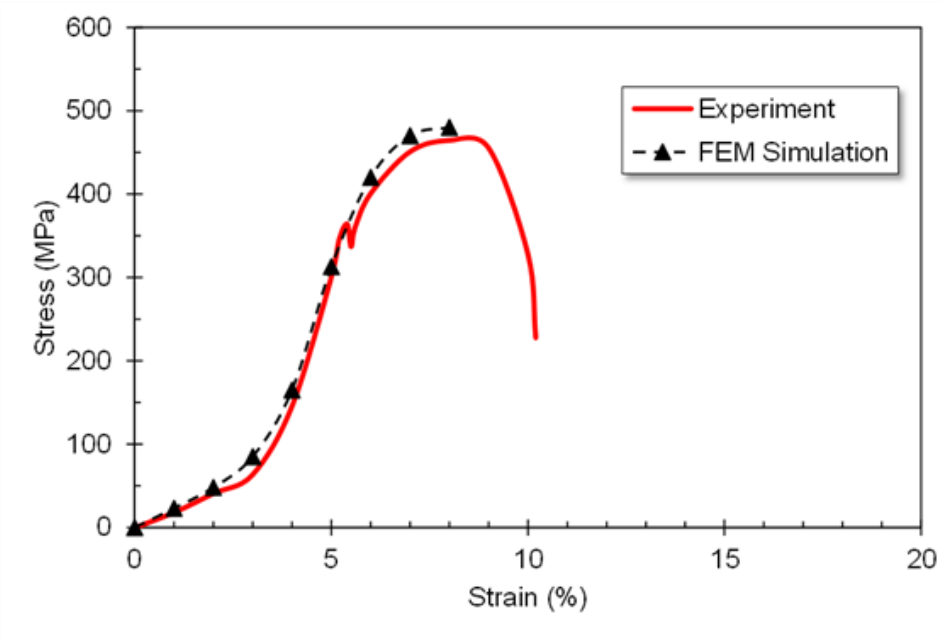

Fig. 13. Validation of FEA simulation with experimental test.

3. RESULT AND DISCUSSION

3.1. Microstructure Hardness Test Results

Hardness testing is carried out using the Vickers microhardness testing technique. Data collection was carried out with a loading of 300 grams. The results of taking the hardness value can be seen in Fig. 14 where referred four color in left side is denoted by A, B, C and D in right side.

Hardness values are measured using the Vickers method, where the measurement process begins at the weld core (in the middle) to the base material so that a straight line is formed. The distance between the data retrieval traces is determined to be 0.25 microns. The data acquisition results can be seen in Fig. 15 and Fig. 16.

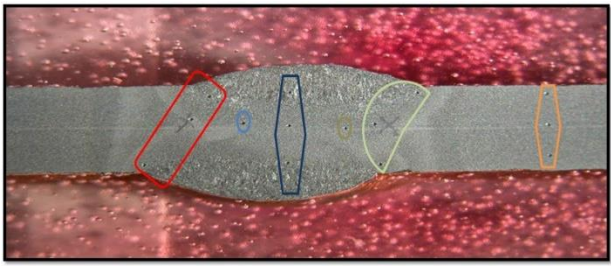

A	B	C	D
133	136	151	136
148	148	148	136
148	144	132	135

Fig. 14. Microhardness measurement results.

Fig. 15. Hardness testing result.

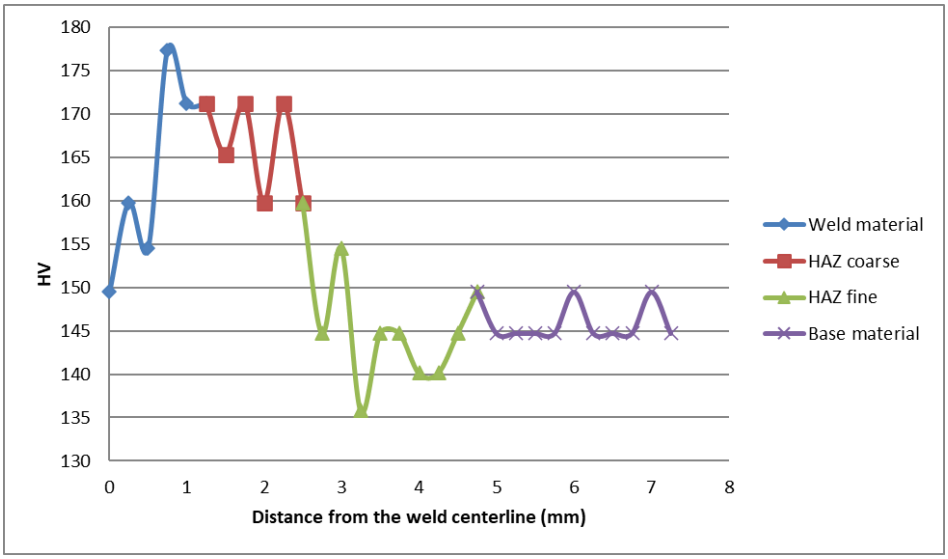

Fig. 16. Micro hardness measurement results.

From the microstructure analysis results, it is found that several areas are generated due to microstructure changes of the material caused by the welding process, which can be mapped by referring to the hardness values of the different test results at the points that have been observed. From these results, data was collected on the hardness value of the material starting from the midpoint, namely the welding material passing through the HAZ area and transitioning to the base material with a distance of 0.25 microns, so that several points formed a straight line with different hardness values, which is consistent with other researcher results [24]. The test results can be seen in the graph at Fig. 16, in which the smallest hardness value is in the fine grain HAZ (Transition) area. The value of the test results is estimated based on the mapped areas so that it can be converted to get the Tensile Strength value by using

estimating formula of TS(Mpa) = 3.45 X HB. From these results, the largest tensile strength value was found in the weld core area of 565.512 MPa, and the smallest Tensile strength area is in the fine grain HAZ area of 497.878 MPa.

3.2. Macroscopic Examination

The macroscopic photos of the cross-section of welding joint can be seen in Fig. 16. It can be seen that the microstructure changes of the welded material can then be mapped into several areas based on the grain structures of the welded material. To make further observations, the circle area is taken a photograph by magnification of 500x. From the picture, it can be seen that the results of the welding process undergo changes in the microstructure caused by the heat given to the welding process [25]. Changes in the microstructure can be seen clearly, so that it can be mapped based on the observations, namely the weld area, coarse grain HAZ, fine grain HAZ and basic material.

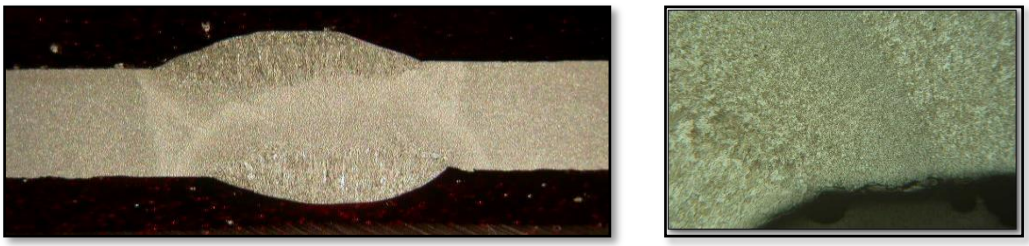

Fig. 17. Macro photos of the welding material.

From the results of distance measurements and macro photos of the welded test objects above, it can be observed that the microstructure changes occurred in the welded specimens which can be mapped into several result areas, namely the Weld Material, HAZ and Base Material areas. In the area between the HAZ and the base material there is a transition region or in other words the fine grain HAZ region which is a critical region. From the mapping of the area resulting from the macro photo, the distance between the welded areas can be measured. The results of the distance measurement can then be modeled into a modeling form using CAD software so that it can be used as material for the next analysis process, namely FEM analysis.

3.3. FEA Simulation Results

Butt Joint modeling is obtained by modeling on Solidworks software; the results can be shown in Fig. 18. The simulation results show that the HAZ area experiences the highest stress concentration compared to that at the base material and weld material areas. It is shown that the stress value at the HAZ area is around 420 MPa, and stress in the Weld Material is around 190 MPa which is the lowest stress. The FEA simulation of the diamond plate model can be seen in Fig. 19.

As shown in Fig. 19 and Fig. 20, the maximum stress of welding plate joint with addition of diamond and circular plates are about 388,26 MPa and 172,67 MPa, respectively. Both maximum stresses occur at the area of weld face reinforcement. However, those maximum stresses do not happen at the predicted critical area, commonly produced by sharp or irregular shapes of machine components which usually generate stress concentration. This indicated that stress-concentration factors do not dominantly control the maximum stress. The bending stress simulation result for base plate without the addition of diamond or circular plates can be seen in Fig. 20. A brief description of bending stress simulation can be seen in Table 2.

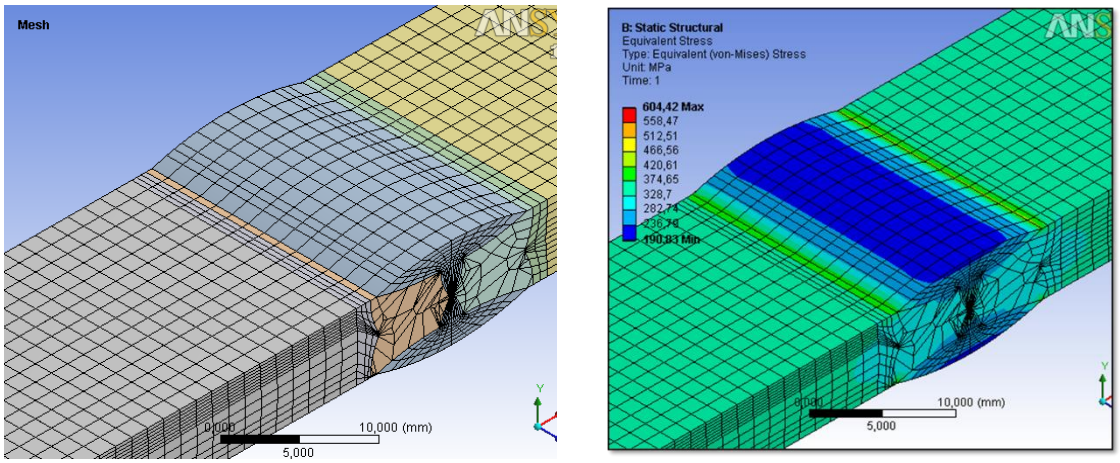

Fig. 18. FEA simulation results.

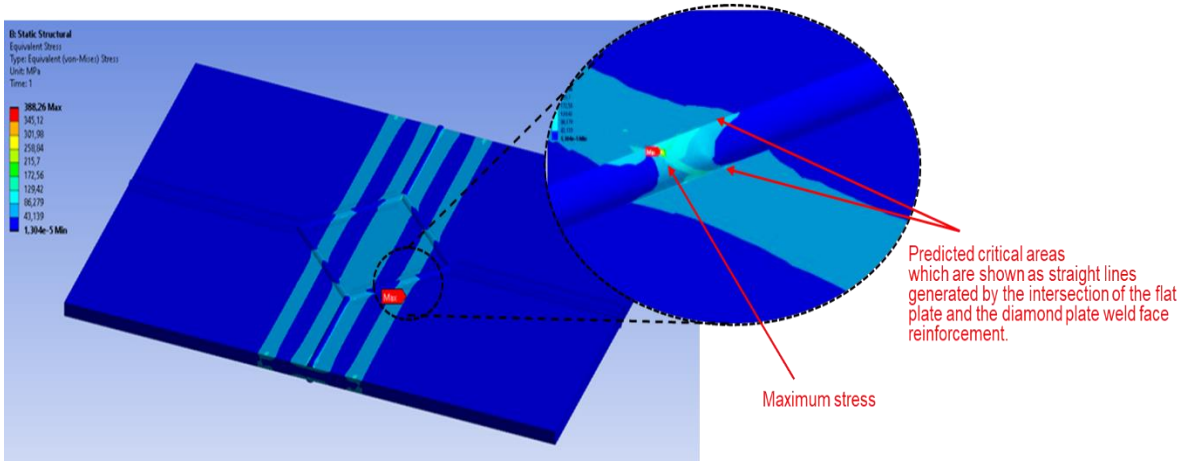

Fig. 19. FEA simulation of the diamond plate model.

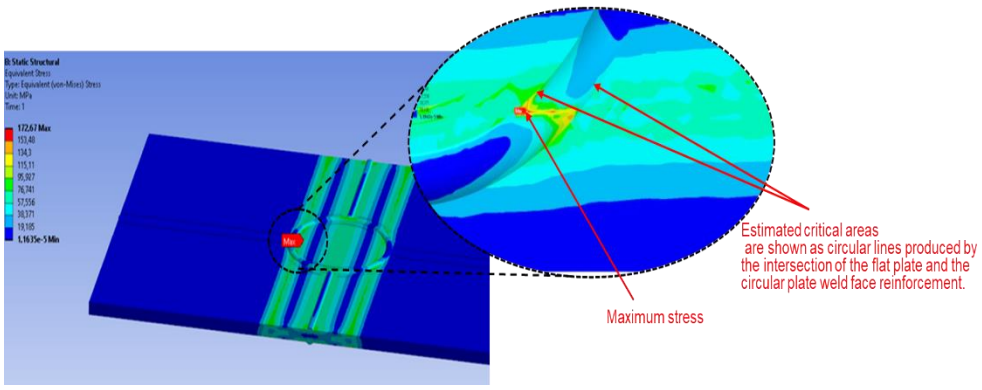

Fig. 20. FEA simulation of the circular plate model.

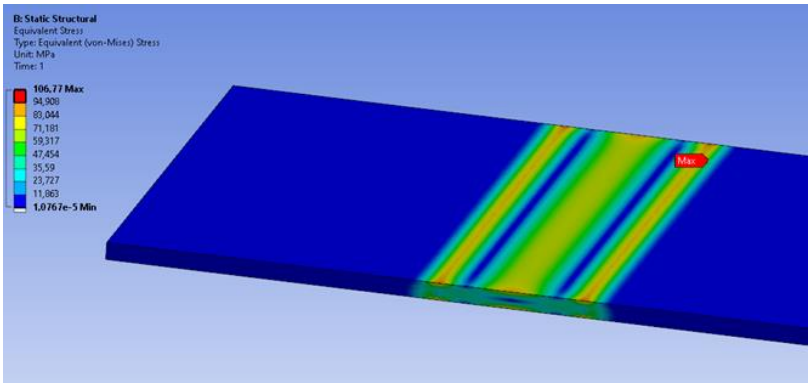

Fig. 21. FEA simulation of the base plate model.

Table 2: Simulation of bending testing using FEM for diamond and circular plates.

No.	Dimension of diamond/ circular plate	Plate thickness	Load	Mesh		Max Stress (MPa)	Additional material on the meeting of plate welding joint
				Element	Node		
1.	60 x 60 mm	6 mm	25 kN	540053	807751	388,26	Diamond
2	∅ = 60 mm	6 mm	25 kN	520460	774043	172,67	Circular
3	Base plate	6 mm	25 kN	526857	781629	106,77	Without additional materials/ base plate only

3.4. Bending and Tension Tests Results

From the mechanical properties testings carried out, it can be analyzed that in the tensile testing, as shown in Fig. 13, the comparison of the ultimate and yield strength is about of 470 MPa / 350 MPa, in other words Ts/Ty is about of 1.3. This is in accordance with ductility requirement of the EN 1993 Eurocode 3 [27] approach, namely Ts / Ty ≥ 1,2. Where, Ts is the ultimate tensile strength, and Ty is yield strength. How to use this document?

The results of bending testing for specimen with diamond and circular plate are shown in Fig. 21. After visually examination on the surface of bending tested specimen, in which the critical area is supposed at weld area, especially fine grain HAZ area. It was found that there were no significant surface damages around welding area for both tested specimen of diamond and circular plates. In other word, both specimens of diamond and circular plates were sucsesfully tested by bending testing, as shown in Fig. 22. Bending test results for plate welding joint with addition of diamond and circular plates as weel as for base plate materials can be seen in Table 3.

Table 3: Bending testing of plate welding joint with an addition of diamond and circular plates.

No	Materials	Shape of additional plate	Specimen Dimension	Thickness	F_{MAX}	Visually surface examination
1	ST 42	Diamond	140x240 mm	6 mm	45,50 kN	No significant surface damages,
2	ST 42	Circular	140x240 mm	6 mm	53,75 kN	No significant surface damages.

Fig. 22. Result of diamond Plate Bending Test.

In addition, maximum load applied to bending test for specimen with an addition of circular plate is about 53,75 kN, and that for diamond plate is about 45,50 kN. This described that maximum load for bending test of circular plate is about 18% greater than that of specimen with a diamond plate, as shown in Table 3. This indicated that the specimen with the addition of circular plate was able to withstand the bending load (bending force) which is about 18% greater than that of the specimen with the addition of a diamond plate.

However, when applying the same load during simulations, the maximum stress of the welding plate joint with the addition of a diamond plate is about 125% greater than that of circular plate, as shown in Table 2. In addition, as shown in Fig. 19 and Fig. 20, the maximum stresses do not occur at supposed critical areas, therefore this can be concluded that the maximum stresses were not dominantly controlled by stress concentration factor, however the maximum stress is strongly affected by the value of section modulus (Z=I/y) of the welding joint structure.

It can be described based on the theory of bending stress in beam, as shown in Equation 1, 2 and 3. The total section modulus of welding joint with an addition of circular plate is greater than that of diamond plate, therefore the maximum stress of welding joint with an addition of circular plate is lower than that of diamond plate. Since, the value of the bending stress is inversely proportional to the section modulus Z.

$$M = \int_A ydP = \int_A y\sigma dA = \frac{\sigma_{max}}{C}\int_A y^2 dA \quad (1)$$

$$\sigma = My/I \quad (2)$$

$$\sigma = M / (I/y) = M/Z \quad (3)$$

Where: M = bending moment, σ = bending stress, I = moment inertia of area, and Z = I/y = section modulus.

4. CONCLUSIONS

From the analysis, it can be concluded as follows:

1. The structure of welded joint material can be mapped into several areas, namely fine grain of HAZ, coarse grain of HAZ, weld material, and base material which is then called as Inhomogeneous Welding Joint Material. The model of inhomogeneous welding materials of double V butt joint was proposed, as shown in Fig. 5.
2. The value of hardness and strength of inhomogeneous material as a result of welding process indicated that the lowest is in the fine grain of HAZ region, and the highest is in the weld material area.
3. The structural integrity of the plate welding joint with the addition of circular plate is greater than that of diamond plate, since it has maximum stress lower than that of diamond plate, and particularly, it can also withstand the maximum bending load Fmax greater than diamond plate.
4. In the viewpoint of application, it can be recommended that plate welding joint with an addition of circular plate is very appropriate for flat deck of ship construction. However, plate welding joints with the addition of diamond plate is mostly recommended for un-flat (cornered) meeting of plate joint structure, because it can fitly joint to the un-flat (cornered) plate joint [26].

ACKNOWLEDGEMENT

Authors would like to express our gratitude to Department of Mechanical Engineering Universitas Indonesia in the providing of support facilities and funding for this research. The authors also would like to acknowledge the Laboratory of Structural Strength, Directorate of Laboratory Management, Research Facilities, and Science and Technology Park - National Research and Innovation Agency, Indonesia, for performing mechanical properties testings.

REFERENCES

[1] X. Meng, Y. Huang, J. Cao, J. Shen, J.F. dos Santos, Recent progress on control strategies for inherent issues in friction stir welding, Prog. Mater. Sci. 115 (2021) 100706. https://doi.org/10.1016/J.PMATSCI.2020.100706.

[2] M. Gierth, P. Henckell, Y. Ali, J. Scholl, J.P. Bergmann, Wire Arc Additive Manufacturing (WAAM) of Aluminum Alloy AlMg5Mn with Energy-Reduced Gas Metal Arc Welding (GMAW), Mater. 2020, Vol. 13, Page 2671. 13 (2020) 2671. https://doi.org/10.3390/MA13122671.

[3] D.K. Dwivedi, Metal Joining: Need, Approaches and Mechanisms, Fundam. Met. Join. (2022) 3–31. https://doi.org/10.1007/978-981-16-4819-9_1.

[4] D. Pathak, R.P. Singh, S. Gaur, V. Balu, Experimental investigation of effects of welding current and electrode angle on tensile strength of shielded metal arc welded low carbon steel plates, Mater. Today Proc. 26 (2020) 929–931. https://doi.org/10.1016/J.MATPR.2020.01.146.

[5] R. Schiller, M. Oswald, J. Neuhäusler, K. Rother, I. Engelhardt, Fatigue strength of partial penetration butt welds of mild steel, Weld. World. 1 (2022) 1–22. https://doi.org/10.1007/S40194-022-01335-Z/TABLES/10.

[6] T.E. Abioye, O.E. Ariwoola, T.I. Ogedengbe, P.K. Farayibi, O.O. Gbadeyan, Effects of Welding Speed on the Microstructure and Corrosion Behavior of Dissimilar Gas Metal Arc Weld Joints of AISI 304 Stainless Steel and Low Carbon Steel, Mater. Today Proc. 17 (2019) 871–877. https://doi.org/10.1016/J.MATPR.2019.06.383.

[7] N. Mukai, Y. Inoue, S. Sasakura, Y. Kinoshita, Prevention of cold cracking by the welding process for reducing diffusible hydrogen in high-tensile thick plate welding,

Https://Doi.Org/10.1080/09507116.2020.1866362. 33 (2021) 268–279. https://doi.org/10.1080/09507116.2020.1866362.
[8] T. Schaupp, M. Rhode, H. Yahyaoui, T. Kannengiesser, Hydrogen-assisted cracking in GMA welding of high-strength structural steels using the modified spray arc process, Weld. World. 64 (2020) 1997–2009. https://doi.org/10.1007/S40194-020-00978-0/TABLES/4.
[9] M. Gáspár, Effect of Welding Heat Input on Simulated HAZ Areas in S960QL High Strength Steel, Met. 2019, Vol. 9, Page 1226. 9 (2019) 1226. https://doi.org/10.3390/MET9111226.
[10] A. Mashhuriazar, C. Hakan Gur, Z. Sajuri, H. Omidvar, Effects of heat input on metallurgical behavior in HAZ of multi-pass and multi-layer welded IN-939 superalloy, J. Mater. Res. Technol. 15 (2021) 1590–1603. https://doi.org/10.1016/J.JMRT.2021.08.113.
[11] K. Zhang, W. Dong, S. Lu, Finite element and experiment analysis of welding residual stress in S355J2 steel considering the bainite transformation, J. Manuf. Process. 62 (2021) 80–89. https://doi.org/10.1016/J.JMAPRO.2020.12.029.
[12] S.H. Li, P. Kumar, S. Chandra, U. Ramamurty, Directed energy deposition of metals: processing, microstructures, and mechanical properties, Https://Doi.Org/10.1080/09506608.2022.2097411. (2022). https://doi.org/10.1080/09506608.2022.2097411.
[13] N. Saba, M. Jawaid, M.T.H. Sultan, An overview of mechanical and physical testing of composite materials, Mech. Phys. Test. Biocomposites, Fibre-Reinforced Compos. Hybrid Compos. (2019) 1–12. https://doi.org/10.1016/B978-0-08-102292-4.00001-1.
[14] T. Patterson, J. Hochanadel, S. Sutton, B. Panton, J. Lippold, A review of high energy density beam processes for welding and additive manufacturing applications, Weld. World. 65 (2021) 1235–1306. https://doi.org/10.1007/S40194-021-01116-0/FIG.S/88.
[15] G. Dak, C. Pandey, Experimental investigation on microstructure, mechanical properties, and residual stresses of dissimilar welded joint of martensitic P92 and AISI 304L austenitic stainless steel, Int. J. Press. Vessel. Pip. 194 (2021) 104536. https://doi.org/10.1016/J.IJPVP.2021.104536.
[16] S. Lin, D. Wang, C. Li, X. Liu, X. Di, Y. Jiang, Effect of cyclic plastic deformation on microstructure and mechanical properties of weld metals used for reel-lay pipeline steels, Mater. Sci. Eng. A. 737 (2018) 77–84. https://doi.org/10.1016/J.MSEA.2018.09.036.
[17] J. Verma, R.V. Taiwade, Effect of welding processes and conditions on the microstructure, mechanical properties and corrosion resistance of duplex stainless steel weldments—A review, J. Manuf. Process. 25 (2017) 134–152. https://doi.org/10.1016/J.JMAPRO.2016.11.003.
[18] S. Tsutsumi, R. Fincato, P. Luo, M. Sano, T. Umeda, T. Kinoshita, T. Tagawa, Effects of weld geometry and HAZ property on low-cycle fatigue behavior of welded joint, Int. J. Fatigue. 156 (2022) 106683. https://doi.org/10.1016/J.IJFATIGUE.2021.106683.
[19] M. Atta, A.A. Abd-Elhady, A. Abu-Sinna, H.E.M. Sallam, Prediction of failure stages for double lap joints using finite element analysis and artificial neural networks, Eng. Fail. Anal. 97 (2019) 242–257. https://doi.org/10.1016/J.ENGFAILANAL.2019.01.042.
[20] R. Beygi, A. Akhavan-Safar, R. Carbas, A.Q. Barbosa, E.A.S. Marques, L.F.M. da Silva, Utilizing a ductile damage criterion for fracture analysis of a dissimilar aluminum/steel joint made by friction stir welding, Eng. Fract. Mech. 274 (2022) 108775. https://doi.org/10.1016/J.ENGFRACMECH.2022.108775.
[21] X. fang Xie, J. Li, W. Jiang, Z. Dong, S.T. Tu, X. Zhai, X. Zhao, Nonhomogeneous microstructure formation and its role on tensile and fatigue performance of duplex stainless steel 2205 multi-pass weld joints, Mater. Sci. Eng. A. 786 (2020) 139426. https://doi.org/10.1016/J.MSEA.2020.139426.
[22] MatWeb, ASTM A572 Steel, grade 42, n.d. https://matweb.com/search/datasheet.aspx?matguid=a1c75a2df3d447c08a8a18ea7be65902 (accessed July 5, 2022).
[23] ANSYS Inc., Ansys Student Workbench-based Simulation Tools, (n.d.). https://www.ansys.com/academic/students/ansys-student (accessed January 9, 2022).
[24] N. das Neves, M.F. Fernandes, C.F. de A. Von Dollinger, J.M.K. Assis, H.J.C. Voorwald, Effects of GTAW Dynamic Wire Feeding Frequencies on Fatigue Strength of ASTM A516-70 Steel Welded Joints, J. Mater. Eng. Perform. 31 (2022) 6435–6450. https://doi.org/10.1007/S11665-022-06868-4/FIG.S/21.

[25] Z. Jiang, D. Liang, T. Zhou, al -, N. Ali, J.K. Hamza, S.E. Sofyan, Effects of welding on the change of microstructure and mechanical properties of low carbon steel, IOP Conf. Ser. Mater. Sci. Eng. 523 (2019) 012065. https://doi.org/10.1088/1757-899X/523/1/012065.

[26] G. Prayogo, E.C. Firdaus, M.A. Budiyanto, Stress analysis of the application of the diamond plate on the quad-joint connection: A case study on the flat plate hull of ships, Http://Www.Editorialmanager.Com/Cogenteng. 9 (2022). https://doi.org/10.1080/23311916.2022.2110705.

[27] Eurocode 3 (EN 1993): Design of steel structures - Part 1-1: General rules and rules for buildings, EN 19931-1, May 2005.